

head the lower the developed friction force. By the results displayed, it is safe to assume that an internal pressure head higher than 0.5 will result in a lower contact length.

The primary goal of vibration analysis is to be able to predict the response, or motion, of a vibrating system (Inman 2001). D'Alembert's Principle states that a product of the mass of the body and its acceleration can be regarded as a force in the opposite direction of the acceleration (Bedford and Fowler 1999). This results in kinetic equilibrium. It is important to note that initially in this vibration study damping of the air, fluid, and material are neglected. Later additions to the dynamic model will include viscous damping and an added mass component. These two additions aid in modeling the behavior of the water in a dynamic state. To adequately represent a model of water in a dynamic system, far too many variables would be needed to consider this behavior. Therefore, to compensate for the complexity of a thorough water model, viscous damping and added mass are introduced. A second feature was added to model the effect of the inertia of the internal water. If the water field oscillates in the same phase as the tube, the translating membrane will behave dynamically as if its mass had increased by that of the vibrating water (Pramila 1987). Moreover, the water particles are assumed to move only in a plane perpendicular to the transverse direction of the tube. However, there is no known precise value for a given fill material and tube property. The added mass component  $a$  is only a coefficient representation of this phenomenon.

Four analytical studies of the geotube's equilibrium response have been performed. Two of these studies employed the use of FLAC while the other two used Mathematica software for a two-dimensional analysis. Huong (2001) selected FLAC to explore the effects of varying the soil characteristics of soft clays. His results included the amount of settlement, tube height, and membrane tension. Kim (2003) also used FLAC to investigate the apron, baffle, sleeved, and stacked tube designs with a Mohr-Coulomb soil model. Her results consisted of finding the critical external water levels, membrane tension, deformations (when loaded externally), and pore pressures. Plaut and Suherman (1997) used Mathematica to develop equilibrium models that considered the effects of submergence, deformable foundation, and impounding water. Specific to this chapter, Plaut and Suherman considered a tensionless Winkler foundation with the tension below the supporting surface not to be constant. Their process in computing equilibrium properties matches the shooting procedure. With the aid of Mathematica, Plaut and Klusman investigated a single tube, two stacked tubes, and a three tube pyramid formation with rigid and modified Winkler foundations (Klusman 1998, Plaut and Klusman 1999). Klusman modified Suherman's Winkler model by assuming a normal foundation force and allowing the tension to be constant along the tube's entire perimeter.

### **Winkler Foundation Model**

A freestanding geosynthetic tube filled with water and supported by a Winkler foundation is being considered. The tube is assumed to be infinitely long and straight catering to a two-dimensional model. Typical assumptions discussed in chapters two and three hold. These assumptions include: longitudinal changes in cross-sectional area are

negligible, geosynthetic material is inextensible, and bending resistance is neglected. Originally proposed by Winkler in 1867, this is the most fundamental foundation model used in many initial analyses. The Winkler foundation model assumes that the downward deflection of the soil at a point is directly proportional to the stress applied at that point and independent of the surrounding soil behavior (Selvadurai 1979). The deflection occurs directly under the load applied. To model this behavior, numerous independent vertical springs are integrated into foundation. The Winkler model has been investigated with problems associated with floating structures (floating bridges and ice sheets), cemented lap joints, and the state of stress at the tip of a crack in an elastic continuum (Selvadurai 1979). When the tube is in contact with the Winkler foundation, tension is not assumed constant. However, above the surface of the Winkler foundation the membrane tension is constant. The internal water is hydrostatically modeled. It is observed that as the soil stiffness increases, the frequencies tend to increase. There is no considerable change in frequency when the soil stiffness is above 25, meaning the stiffer the soil, the less effect it has on the frequency.

### **Pasternak Foundation Model**

A long freestanding geosynthetic tube filled with water and supported by a Pasternak foundation is considered. The general assumptions of the geosynthetic tube remain the same as before. Pasternak in 1954 extended the Winkler model by adding a shear layer to the vertical springs. The primary difference between the Winkler and Pasternak foundation models is the presence of the shear interaction layer between the Winkler spring elements. This shear layer is composed of incompressible vertical elements which deform in the transverse shear direction only (Selvadurai 1979). The results from this model should more closely approach what actually occurs in a real world application. It was observed that when the soil stiffness parameter is increased to 200 the shear modulus has little effect, if any, on the initial tension. As the shear modulus is increased, tube settlement decreases. This situation is expected. When the soil on a supporting surface has the ability to rely on the surrounding soil for a broader stress distribution, then the tube settlement should decrease appropriately. Tube height above the Pasternak foundation surface does not change significantly as a function of the soil's shear modulus. If the soil stiffness coefficient is held at 200, then the Pasternak foundation mode shapes are identical to the Winkler foundation mode shapes, with the exception of varying with the shear modulus. For given internal pressure heads  $h = 0.2, 0.3, 0.4, \text{ and } 0.5$ , the lowest four natural frequencies conform to the curves displayed in the following frequency to shear modulus graphs. A decrease in frequency occurs when the shear modulus  $g_p$  is increased. Physically, the number of times the mode shapes passes through the equilibrium configuration for a given range of time decreases slightly.

Once the equilibrium program was executed (with respect to the designated internal pressure head or internal air pressure) and the results of contact length and initial membrane tension were calculated, vibrations about the equilibrium configuration may be introduced. Set values for the dynamic computations for both the internal water and air cases include: the internal pressure head ( $h$ ) or air pressure ( $p$ ), contact length of

tube/surface interface, and membrane tension at the origin. These equilibrium properties were used to solve for unknown parameters (for example, the dynamic tension parameter

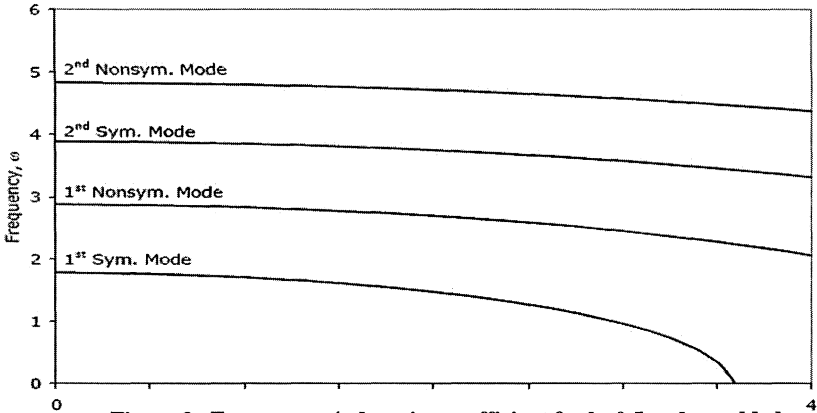


Figure 3. Frequency v/s damping coefficient for  $h=0.5$  and no added mass

$q_0$ ), the natural frequencies, and the mode shapes.

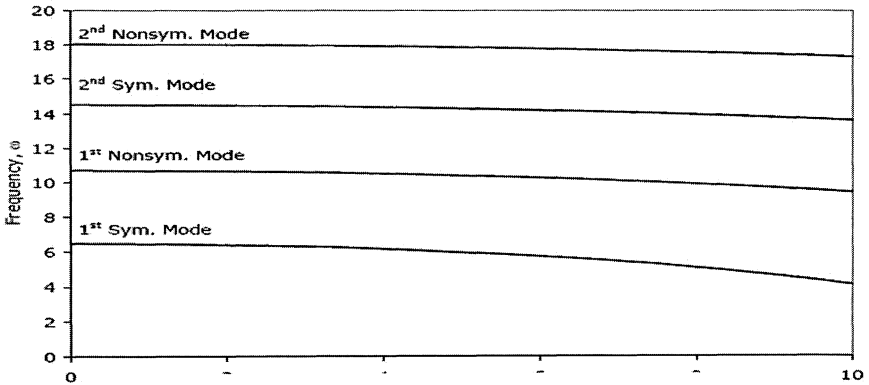


Figure 4. Frequency v/s damping coefficient with  $p=5$

**Conclusions**

The largest value of tension occurs primarily at the highest internal pressure head. This translates into needing a more durable material that has enough tension capacity to withstand the expanding of the membrane that an increase in pressure head would cause. Though the water and air results are not directly comparable, this trend of increasing membrane tension as the internal pressure rises is maintained within each of

the six cases considered: internal air and water tubes resting on rigid, Winkler, and Pasternak foundations. The four frequencies and corresponding mode shapes are classified by the number of intersection points or nodes that are present between the equilibrium configuration and dynamic shape. Thus, the First symmetrical mode possesses two nodes, next the First nonsymmetrical mode has three nodes, the Second symmetrical mode has four nodes, and lastly, the Second symmetrical mode has five nodes. The frequencies will decrease or increase by adjusting the internal pressure head or internal air pressure, damping coefficient, added mass multiplier (where applicable), soil stiffness coefficient, and the shear modulus. Focusing on the deformable foundation models, the frequency tends to increase as the soil stiffness increases, but decreases as the shear modulus increases. It stands to reason that a tube on a vertically stiffened soil (without the presence of transverse soil interaction) will tend to vibrate faster than on the same soil with the presence of transverse soil interaction (i.e., shear modulus).

Though the dimensional comparison of rigid foundation equilibrium and dynamic results of water and air did not correlate well regarding tension, tube settlement, and tube height above the supporting surface, the difference can be reasoned. Since the geosynthetic material is assumed to be inextensible, the demand for internal air pressure is only that of raising the weight of the tube material. In contrast, the water-filled case needs water to expand in all directions in order to fill the tube's cross-section in its entirety with water, and has relatively large downward components of pressure near the bottom of the tube. The problem also lies with the combination of neglecting the weight of the material in the water-filled case and assuming that the material is inextensible. Therefore, the air and water-filled results are incompatible and are two independent models. With the addition of damping, the dynamic results for both the rigid foundation with air and with water shared the general trend of a curved downward transition to where the oscillation died out. Overall the general shapes for the four modes computed share both the number of nodes (intersection points with the equilibrium configuration) and dynamic shape, considering the tube settlement involved with the deformable foundations.

The analysis of anchored tubes provided the same deformation patterns observed in freestanding tube, but stability of system increased. The further enhancement was provided by using strapping system, which prevented rolling, sliding and toppling of gnotubes under very high hydrodynamic loads.

One aspect for further study would be to see an applied external load such as marine water or debris, and how the dynamic response is affected. Regarding a simulation, it would be good to see a total model incorporating various foundation theories and combined mode shapes. A dimensional solution should be computed for comparison to physical experiments that would investigate equilibrium properties (membrane tension and geometry), dynamic response (geometry), and various soil parameters (soil stiffness and shear modulus). A three-dimensional analysis, possibly using the finite element method, could produce useful results.

## References

- Austin, T. (1995). "A second life for dredged material." *Civil Engineering*, ASCE, Vol. 65, No. 11, pp. 60-63
- Bedford, A, and Fowler, W. (1999). *Engineering Mechanics: Dynamics*, 2<sup>nd</sup> ed. Addison-Wesley, Berkeley, CA.
- Biggar, K., and Masala, S. (1998). *Alternatives to Sandbags for Temporary Flood Protection*, Alberta Transportation and Utilities, Disaster Services Branch and Emergency Preparedness Canada, Edmonton, Alberta.
- Erchinger, H.F. (1993). "Geotextile tubes filled with sand for beach erosion control, North Sea Coast, Germany." *Geosynthetics Case Histories*, G. P. Raymond and J.-P. Giroud, eds., BiTech Publishers, Richmond, BC, Canada, 102-103.
- Freeman, M. (2002). *Experiments and Analysis of Water-filled Tubes Used as Temporary Flood Barriers*, M. S. Thesis, Virginia Tech, Blacksburg, VA.
- Hsieh, J.-C., and Plaut, R. H. (1990). "Free vibrations of inflatable dams," *Acta Mechanica*, Vol. 85, pp. 207-220.
- Huong, T. C. (2001). *Two-Dimensional Analysis of Water-Filled Geomembrane Tubes Used As Temporary Flood-Fighting Devices*, M. S. Thesis, Virginia Tech, Blacksburg, VA.
- Inman, D. J. (2001). *Engineering Vibration*, 2<sup>nd</sup> ed. Prentice Hall, Englewood Cliffs, New Jersey.
- Klusman, C. R. (1998). *Two-Dimensional Analysis of Stacked Geosynthetic Tubes*, M. S. Thesis, Virginia Tech, Blacksburg, VA.
- Kim, M. (2003). *Two-Dimensional Analysis of Different Types of Water-filled Geomembrane Tubes as Temporary Flood-Fighting Devices*, Ph. D. Dissertation, Virginia Tech, Blacksburg, VA.
- Koerner, R. M., and Welsh, J. P. (1980). "Fabric forms conform to any shape." *Concrete Construction*, Vol. 25, pp. 401-409.
- Landis, K. (2000). "Control floods with geotextile cofferdams," *Geotechnical Fabrics Report*, Vol. 18, No. 3, pp. 24-29.
- Plaut, R. H., and Klusman, C. R. (1999). "Two-dimensional analysis of stacked geosynthetic tubes on deformable foundations," *Thin-Walled Structures*, Vol. 34, pp. 179-194.
- Liapis, S. I., Plaut, R. H. and Telionis, D. P. (1998). "When the levee inflates." *Civil Engineering*, ASCE, Vol. 68, No. 1, pp. 62-64.
- Plaut, R. H., and Suherman, S. (1998). "Two-dimensional analysis of geosynthetic tubes," *Acta Mechanica*, Vol. 129, pp. 207-218.
- Pramila, A. (1987). "Natural frequencies of a submerged axially moving band." *Journal of Sound and Vibration*, Vol. 113, pp. 198-203.
- Scott, R. F. (1981). *Foundation Analysis*. Prentice-Hall, Englewood Cliffs, NJ.
- Seay, P. A., and Plaut, R. H. (1998). "Three-dimensional behavior of geosynthetic tubes." *Thin-Walled Structures*, Vol. 32, pp. 263-274.
- Selvadurai, A.P.S. (1979). *Elastic Analysis of Soil-Foundation Interaction*. Elsevier, New York.
- Wolfram, S. (1996). *The Mathematica Book*, 3<sup>rd</sup> ed., Cambridge University Press, Cambridge, UK.

## Slamming Forces due to Random waves on Horizontal Circular Members in Intertidal Zone

V. Hariprasad<sup>1</sup>, R. Sundaravadeivelu<sup>2</sup> and S. Neelamani<sup>3</sup>

<sup>1,2</sup>Ocean Engineering Department, Indian Institute of Technology Madras, Chennai-600036, India; email: [vhariprasad\\_iitm@yahoo.co.in](mailto:vhariprasad_iitm@yahoo.co.in)

<sup>3</sup>Coastal Engg. and Air Pollution Dept, Environmental and Urban Development Division, Kuwait Institute for Scientific Research, P.O. Box : 24885, 13109, Safat, Kuwait; email: [nsubram@safat.kisr.edu.kw](mailto:nsubram@safat.kisr.edu.kw)

### *Abstract*

Wave forces acting on slender cylinders are normally estimated using Morison equation (1950). When a structural member is near the free water surface, it experiences the slamming force. Wave slamming on horizontal members of any ocean structure is crucial to its design. API Recommended Practice 2A-WSD (2000) recommends slamming coefficient  $C_s$  equal to  $\pi$  for circular cross sectional members near the still water level. The horizontal cylinders in the inter tidal zone for Port craft jetties are subjected not only to slamming force in the vertical direction and horizontal direction but also berthing force in the horizontal direction. If two cylinders are kept in close spacing, then the load on each member will be different compared to force on a single member kept alone. In this paper, the results of investigations of the effect of tidal variation on slamming forces are reported. The comparison of single circular member and twin circular members with c/c spacing varying from two to four times the diameter of cylindrical member in random waves is also included in this paper. The slamming coefficient is found to be not a constant value and it varies with respect to the spacing between the cylinder and free water surface, the incident wave height and wave period.

### *Introduction*

Experiments are conducted for single circular and double circular cross sectional shapes of the cylinders. The horizontal and vertical forces on different cylinders are measured by keeping the distance between the flume bed and centre of the member constant and by varying the water depth (d) for various hydrodynamic conditions.

The main purpose of this investigation is to study the effect of wave height, wave frequency, the distance between the free water surface and the centre of the member etc. on the vertical slamming coefficient ( $C_{sv}$ ) and the horizontal slamming

coefficient ( $C_{sh}$ ). The results of this investigation can be used for the hydrodynamic design of horizontal members in the intertidal zone for any ocean structure. This paper includes the wave slamming forces on single circular cylinder and twin circular cylinder models due to random waves.

For experimental investigations on the cylinders random waves are generated in a wave flume of 30m length, 2m wide and 1.7m depth in the Department of Ocean Engineering Indian Institute of Technology, Madras, India.

### *Literature review*

There are studies carried out on wave slamming forces around a single circular cylinders kept closer to the free water surface and in the wave field. But the investigations did not cover a large range of input conditions and hence warrants the present work.

The impact force is defined as the rate of change of momentum associated with mass of water moving past the structure. When the fluid makes a contact with the structure, the water particle in the vicinity of the structure undergoes large accelerations. Experimental and theoretical works from previous literatures [1 to 9] has a wide scatter of  $C_s$  from 1.0 to 7.79 and experiments have done by dropping the cylinder to calm water

*Dalton et al* (1976) has investigated the slamming forces on the horizontal member fixed in the splash zone. The slamming coefficients obtained experimentally were reported to vary from 1.0 to 4.5. The variation of  $C_s$  with  $KC$  for different wave periods and at different submergence levels was reported.

*Faltinsen et al* (1977) has investigated forces on the members of the ocean structure in the free water surface zone. The theoretical calculations are compared with experimental results obtained by forcing rigid horizontal circular cylinders with constant velocity through an initially calm free surface. Numerically estimated slamming coefficient was 3.1. Experiments gave an average  $C_S$  of 5.3.

*Garrison* (1996) investigated the impact loads on circular members both experimentally and theoretically. A new design method for computing stresses in cylindrical members due to impact is developed based on the energy principle showing well agreement with the experiments. He obtained stress equations from the energy principle for the design purposes for the first peak in the stress curve and steady state stress. From the test data, it is seen that stress in the transition region is equal to or less than the steady state stress.

*Graham Dixon et al* (1979) showed that for partially submerged cylinders, varying buoyancy could play as large a part as inertial force. Morison's equation has been adopted to predict the effects for regular waves by introducing a varying volume and a buoyancy term. It is also shown that a constant value for  $C_M$  equal to 2 can be used as a design constant. For small values of wave amplitude and wave steepness the agreement with experiment is made fairly well by fitting the inertial coefficient to each of the experimental curves.

*Kaplan et al* (1976) presented a mathematical model for determining time histories of vertical impact forces on platform horizontal structural members in the splash zone.

Plots showing the variation between the rates of change of added mass with depth of immersion are shown.

*Martin et al* (1983) studied experimentally and theoretically the scattering of regular surface waves on a fixed, half immersed circular cylinder, which is partially reflected and partially transmitted and also induces hydrodynamic forces on the cylinder. These horizontal and vertical coefficients are compared with the linear theory and found that former was accurately predictable even for large waves and latter was predictable only for small amplitude waves.

*Miyata et al* (1990) made an experimental and numerical study of forces and flow about a circular cylinder steadily advancing beneath the free surface. Here flow visualization also used to know the difference of vortex shedding due to the difference of the depth of submergence. This results in a smaller pressure reduction on the backward face of the cylinder and a lower value of  $C_D$ .

*Sarpkaya* (1978) estimated wave forces acting on horizontal cylinders subjected to impact both theoretically and experimentally. The results have been expressed in terms of two force coefficients one slamming coefficient at the time of impact and another drag coefficient when cylinder is immersed approximately 1.8 times diameter inside water. It is found that at initial instants of impact,  $C_S$  is very close to the theoretical value of  $\pi$ . Also it is found that  $C_S$  may be amplified to a value as high as 6.3 through the dynamic response of the cylinder.

A detailed investigation of slamming forces on single horizontal cylinder for wide range of tidal variation is not available in the literature. Also studies on twin cylinders in the flash zone are not given much attention so far, which has motivated the authors to carryout this work.

### **Experimentation procedure, model description and instrumentation**

Figure 1 is the definition sketch of the present problem. The experimental investigations were carried out using a 0.063m diameter circular cylinder model with two load cells fixed at the two ends in a varying water depth as 0.4m, 0.45m, 0.50m, 0.55m, and 0.6m. The end portions were air tightened with rubber sheets and perspex in order to prevent the entry of water inside the cylinder.

The experimental investigation was carried out first for single circular cylinder, which is taken as a reference for the force variation in the twin circular cylinder

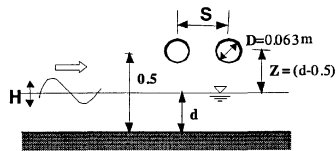


**Fig. 1 Definition sketch**

The different ranges of the normalized hydrodynamic parameters obtained are shown in Table 1.

**Table 1 Ranges of the hydrodynamic parameters**

Parameters	circular cylinder (Dia=0.063m)
Incident wave steepness, $H_s/L_p$	0.011 - 0.058
Relative water depth, $d/L_p$	0.066 - 0.299
Normalized wave height, $H_s/D$	1.128 - 2.425
Relative level of submergence, $z/D$	-1.59 - +1.59
Scattering parameter, $D/L_p$	0.009-0.034
Keulegan- Carpenter number (KC)	3.76 - 18.08
Effective spacing between the cylinders for twin circular case ( $S/D = 0$ for single cylinder case)	2, 4 & 6

The circular cylinder model is fabricated using aluminium with outer diameter ( $D$ ) of 0.063m and thickness of 3mm. Length of the cylinders is kept as 1.89m. The distance between the cylinder centre and the flume bed is kept constant height ( $h$ ) as 0.5m. The model was located at a distance of 11m from the wave generator and 19m from the rubble beach, which is located at the tail end of the flume.

To measure the wave forces on the cylinders, two-component strain gauge type load cells of two numbers of capacity 300N each were fixed at the two ends of the cylinders. This load cell is capable of measuring forces in the horizontal ( $X$ ) and vertical ( $Z$ ) directions. Maximum force of the order of about 90N was measured. These load cells were fixed to the ends the cylinders by providing proper seals made of very thin rubber sheets to prevent the entry of water into the cylinder. Final alignment of the load cell was based on the elimination of vertical force channel output when the load cell was loaded in the horizontal direction, and vice-versa. Calibration was done by applying weights to the model fixed with load cell which is mounted in the framework in the expected principal wave force component directions.

A wave probe is fixed 9m away from the wave maker at the upstream side to measure the incident wave history ( $\eta_1$ ). Three more wave probes are used in the study. One to measure the inline water surface fluctuation on the first cylinder ( $\eta_2$ ) at its leading edge and one to measure the water fluctuation in between the two cylinders ( $\eta_3$ ) and third one to measure the inline water surface fluctuation on the rear cylinder ( $\eta_4$ ) at its trailing edge. Standard Conductance type (two parallel stainless steel electrodes with 2-cm distance between them) wave gauges were used for the measurements of incident and inline wave fields. The natural frequency of the model cylinder with setup is found experimentally to be 44Hz. Random waves were generated for 60sec and the data were collected for 60sec at a sampling rate of 40 Hz.

## Results and discussion

### General

The present experimental investigations on wave loads on the horizontal circular members were carried out mostly in the drag-dominated region. The slamming force in the horizontal and vertical directions can be estimated as

$$F_{sh} = \frac{1}{2} \times C_{sh} \times \rho \times A_p \times u^2$$

$$F_{sv} = \frac{1}{2} \times C_{sv} \times \rho \times A_p \times u^2$$

where

$F_{sh}$  : The slamming force in the horizontal direction

$F_{sv}$  : The slamming force in the vertical direction

$C_{sh}$  : The slamming coefficient in the horizontal direction

$C_{sv}$  : The slamming coefficient in the vertical direction

$\rho$  : The water density

$A_p$  : The projected area of the member normal to the plane of impact, which is equal to  $D$  per unit length of the circular cylinder

$u$  : The horizontal water particle velocity at SWL in the wave field

The measured slamming coefficient is determined using threshold crossing analysis of the force time series. From the horizontal force time series shoreward and seaward forces were obtained. Similarly from the vertical force time series upward and downward forces were obtained. The notations for the coefficients for the upstream (u/s) and downstream (d/s) cylinders are shown below

$C_{sh1}$  : horizontal slamming coefficient in the u/s cylinder

$C_{sv1}$  : vertical slamming coefficient in the u/s cylinder

$C_{sh2}$  : horizontal slamming coefficient in the d/s cylinder

$C_{sv2}$  : vertical slamming coefficient in the d/s cylinder

When the body becomes more immersed, buoyant force will be more predominant. Here in the present experiment in the still water condition itself it is reduced so that the obtained vertical force will be buoyant force excluded.

For experimental investigations Pierson-Moskowitz spectrum had been used for the generation of irregular sea state in the flume. Using the ws4 package wave time series has been generated in the flume by using inverse FFT technique. After acquiring the data, the wave and force spectrum is drawn for the single cylinder case alone that is shown in figure 2.